EUROFUSION WPS1-PR(16) 15197

N Tamura et al.

Tracer-Encapsulated Solid Pellet (TESPEL) Injection System for the TJ-II stellarator

Preprint of Paper to be submitted for publication in
21st Topical Conference on High Temperature Plasma
Diagnostics 2016

Tracer-Encapsulated Solid Pellet (TESPEL) Injection System for the TJ-II stellarator[a]

N. Tamura[1,b], K. J. McCarthy[2], H. Hayashi[1], S. K. Combs[3], C. Foust[3], R. García[2],
N. Panadero[2], E. Pawelec[4], J. Hernández Sánchez[2], M. Navarro[2], A. Soleto[2] and
TJ-II team[2]

[1]*National Institute for Fusion Science, 322-6 Oroshi-cho, Toki-shi, Gifu 509-5292, Japan*
[2]*Laboratorio Nacional de Fusión, CIEMAT, Av. Complutense 40, Madrid 28040, Spain*
[3]*Oak Ridge National Laboratory, 1 Bethel Valley Road, Oak Ridge, Tennessee 37831, USA*
[4]*Institute of Physics, Opole University, ul. Oleska 48, Opole 45-052, Poland*

(Presented XXXXX; received XXXXX; accepted XXXXX; published online XXXXX)

A tracer-encapsulated solid pellet (TESPEL) injection system for the TJ-II stellarator was recently developed. In order to reduce much the time and cost for the development, we combined a compact TESPEL injector provided by National Institute for Fusion Science with an existing TJ-II cryogenic pellet injection system. Consequently, the TESPEL injection into the TJ-II plasma was successfully achieved, which was confirmed by several pellet diagnostics including a normal-incidence spectrometer for monitoring a tracer impurity behavior.

I. INTRODUCTION

In the research of magnetically confined high temperature plasmas aiming for establishing a fusion reactor, impurity transport is one of the critical issues to be clarified. In order to promote a definitive study of impurity transport in the magnetically confined plasma, a Tracer-Encapsulated Solid Pellet (TESPEL)[1] has been developed at National Institute for Fusion Science in Japan. Simply stated, the TESPEL is a double-layered impurity pellet. Usually, the outer layer of the TESPEL consists of a polystyrene $(C_8H_8)_n$ polymer and the tracer impurity is embedded in the inner core. Owing to this configuration, the TESPEL can deposit the tracer impurity within a three-dimensionally limited region in the plasma.[2] The recent LHD experiment with the TESPEL method suggests the importance of a location (inside/outside a last-closed flux surface) of the impurity source on impurity behavior in the plasma.[3] As a result of acquiring such new knowledge including a poloidally asymmetric distribution of the impurities[4], the importance of the comprehensive study of impurity transport is increasingly recognized. A common experimental tool would accelerate the comprehensive study with multi-machine experiments, because it could reduce ambiguity in the results. Consequently, it was agreed to install the TESPEL injection system on the TJ-II stellarator.

This paper describes the TESPEL injection system, which was recently developed for the TJ-II stellarator. In Sec. II, the set-up for the TESPEL injection system is given. In Sec. III, the first results with the developed system are presented. In Sec. IV, lessons learned from this development and future work in the TESPEL injection experiment on TJ-II are shown.

II. SET-UP FOR THE TESPEL INJECTION SYSTEM

A. TJ-II Stellarator

The TJ-II is a 4-period, low magnetic shear, stellarator device with an average minor radius of ≤ 0.22 m and a major radius of 1.5 m.[5] It was designed to explore a wide range of rotational transforms [$0.9 \leq i(0)/2\pi \leq 2.2$]. Its magnetic field is generated by a system of poloidal, toroidal and vertical field coils, and the resultant cross-section of its fully 3-dimensional plasma structure is bean shaped with magnetic field $B(0) \leq 1$ T. For this work plasmas, with hydrogen as the working gas, were created and maintained using electron cyclotron resonance heating (P_{ECRH} ~500 kW). Additional heating was provided by a neutral beam injector (P_{NBI} ~310 kW, $V_{NBI} = 25$ keV, $t_{NBI} \leq 100$ ms). As a result, plasmas with central electron densities, $n_e(0)$, $\leq 2\times10^{19}$ m^{-3} and temperatures, $T_e(0)$, ≤ 800 eV were achieved with a lithium coating on the vacuum vessel wall.

B. TESPEL

The size and contents of the TESPEL are flexible, which is one of the unique features of the TESPEL. In LHD, the size of the TESPEL ranges from 400 μm to 900 μm, depending on the intended use. And as to the contents of the TESPEL, 34 kinds of elements have been used so far for the study of impurity transport and atomic, molecular physics. Since the plasma size of the TJ-II stellarator is similar to that of the Compact Helical System (CHS)[6], which was utilized for the proof-of-principle experiment of the TESPEL, the size of TESPEL for the TJ-II could be similar to that for the CHS: the outer and inner diameters of the TESPEL are about 300 μm and 100 μm, respectively. As the tracer material, although lithium (Li, Z = 3) was used for the CHS in the form of lithium hydride (LiH), aluminum (Al, Z = 13) was selected for the TJ-II in view of the frequent usage of lithium for wall conditioning in the TJ-II. In this case, the particle amounts supplied to the TJ-II plasma are expected as follows: carbon from the shell: 6.7×10^{17}, Al as the tracer: 3.2×10^{16}, electron: 4.7×10^{18} from the shell and 4.1×10^{17} from the tracer.

---

[a] Contributed paper published as part of the Proceedings of the 21st Topical Conference on High-Temperature Plasma Diagnostics (HTPD 2016) in Madison, Wisconsin, USA.

[b] Author to whom correspondence should be addressed:
ntamura@LHD.nifs.ac.jp.

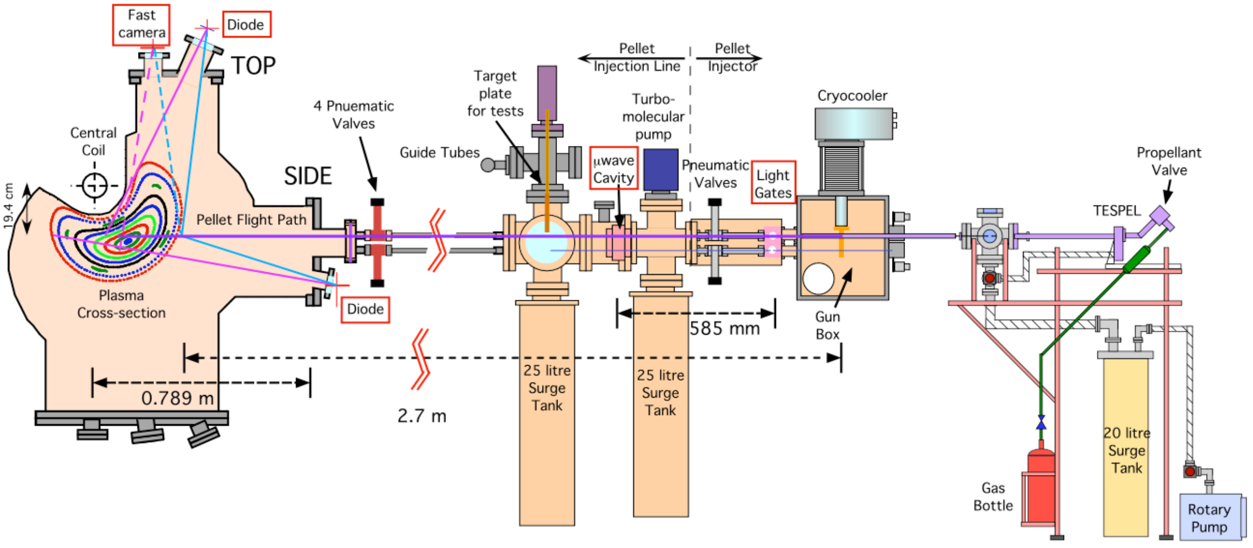

FIG. 1: Sketch of TJ-II toroidal sector B2 with the pellet injector and the TESPEL system.

C. Pellet Injector Modifications

A cryogenic pellet injector (PI) has been operated on the TJ-II since 2014. Its acceleration, guide line diagnostics, delivery and control systems were developed, built and tested at the laboratories of the Fusion Energy Division of Oak Ridge National Laboratory, Tennessee, USA before being installed on TJ-II.[7] A schematic of the pellet injection system is found in Fig. 1. The system consists of a gun box in which pellets are created at 10 K and a gas propellant system for pellet acceleration. Closer to TJ-II, the injection line is equipped with two diagnostics through which pellets pass before reaching TJ-II. The first consists of a light emitting diode and a light sensitive diode (light gates) to provide a time signal. The second is a microwave cavity mass detector. It provides a second timing signal whose amplitude is mass dependent thus facilitating particle accountability.

For these TESPEL tests, one of the cryogenic pellet formation pipes and its gas propulsion system were removed from the PI gun box. This provided a means to directly couple the TESPEL system to the TJ-II PI system thereby taking advantage of the in-line timing, gas expansion and vacuum systems. For this a ~1.3 m long slightly curved guide tube (1.4 mm inner diam.) was used to vacuum couple the upstream end of the corresponding PI guide tube to the downstream end of the TESPEL chamber as indicated in Fig. 1. Note: a slightly curved tube was needed because of nearby space limitations. Also, a custom designed table was used to support the TESPEL and to permit vertical displacement adjustments to be made. In addition, an independent rotary pump vacuum system and an additional 25-litre gas expansion volume were provided for the TESPEL. Finally, timing and control signals for TESPEL injection were achieved by modifying the PI control system.

D. Pellet and Plasma Diagnostics

In order to record the light emitted from the neutral cloud surrounding the TESPEL as it penetrates into the plasma, optical fiber based diagnostic systems have been installed outside nearby upper (TOP OUTER) and rear (SIDE) optical viewports, as shown in Fig. 1. These incorporate a 5 m long, 600 µm diameter optical fibers (model M34L05), and narrowband pass filters (models FB660-10 and FB400-10). The selected filters have central wavelengths at 660 nm +/-2 nm and 400 nm +/-2 nm, for recording Balmer Hα light (λ = 656.28 nm) and Al I light (λ = 394.4 and 396.1 nm), respectively. Both filters have a full-width at half-maximum (FWHM) of 10 +/-2 nm. Note: lenses are not used as the acceptance angle of the fiber (with respect to TESPEL flight path) is ~27° FWHM which allows light to be collected along the whole ablation path (≤0.4 m). The light is measured using a switchable gain, amplified silicon photodiode detectors (model PDA36A), (all by Thorlabs, Newton, NJ) and an avalanche photodiode (APD), (model LCSA3000-01 by Laser Components GmbH, Olching, Germany). As a TESPEL crosses the plasma outer minor radius in ≤5 ms, the detector bandwidth is set to a few 100's of kHz. In this way, it is possible to follow the temporal evolution of the TESPEL ablation by analysing light emissions from the neutral cloud. Finally, for data acquisition a 12-bit, ultra high-speed multifunction board with 4 analogue inputs and 20 Msamples/s sampling rate capability is used (model PCI-DAS4020/12 by Measurement Computing Corporation, Norton, MA). It is located in a nearby PC that automatically transfers data to the TJ-II data base system.

In parallel, an ultra-fast frame CMOS-camera was used to obtain multiple images of the TESPEL cloud (model APX-RS by Photron Incorp., San Diego, CA), from a second upper (TOP INSIDE) optical viewport. Light was collected and transmitted to this camera using a machine-vision type camera lens (*e.g.* model HF16SA-1 by Fujinon, Tokyo, Japan) and a bifurcated coherent fiber bundle (by Schott AG, Mainz, Germany). The camera, which has 2 Gbytes of digital memory, can record between 3×10^4 (1024×1024 pixels) and 2.5×10^5 (128×16 pixels) frames per second. Recorded images are used to study TESPEL deflection and acceleration, cloud shape, asymmetry and elongation, and cloud drift. No light filter was used with this system.

III. RESULTS

During TESPEL evaluation on TJ-II, 26 pellets (300 µm outer diam.), with and without aluminum tracer, were launched into ECRH and/or NBI heated plasmas created using a range of magnetic configurations (100_24_58 to 100_54_67), where the nomenclature reflects currents in the central, helical and vertical field coils, respectively.[9] Of these, 14 intact pellets, with average velocity of 200 m/s +/-40 m/s, reached the plasma edge. A representative ablation light profile is presented in Fig. 2. It is

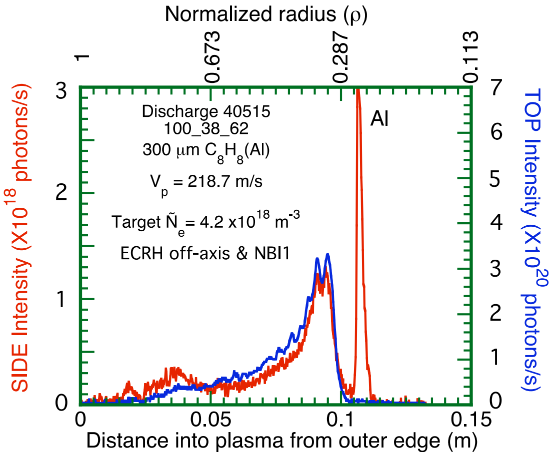

FIG. 2. Hα (blue) and Al I (red) light from ablation of a 300 μm TESPEL entering the TJ-II plasma. Note: Hε light (λ = 397 nm) leaks through SIDE filter. The photon emission rate is estimated to be ~0.02 photon/pellet particle/e.[8] Plasma details are included in the figure.

seen that the aluminum tracer is deposited at ~0.1 m from the plasma edge, *i.e.*, at normalized radius ρ = 0.25.

The response of the plasma to a TESPEL injection is seen in Fig. 3. Immediate cooling at all plasma radii plus a jump in line-averaged electron density, $\tilde{N}_e$, is seen. This is followed by a slow evolution of $\tilde{N}_e$ to a maximum ~5 ms later and a preferential recovery of central T_e. The maximum in $\tilde{N}_e$ equates to 4×10^{18} additional electrons, compared to an estimate of 4.7×10^{18} electrons from the polystyrene and aluminium atoms. Thus, for a low target $\tilde{N}_e$ the plasma does not reach cut-off, rather it cools and recovers.

Spectra collected (every 3.84 ms) using a normal-incidence spectrometer indicate that the tracer is ionized up to Al^{+9} (See Fig. 4). Preliminary analysis of spectral line evolution along the same discharge provides an impurity confinement time of the order 13.6 ms in this low-density TJ-II plasma. This is similar to values obtained using the laser blow-off technique.[10]

IV. DISCUSSION

We have developed the TESPEL injection system on the TJ-II stellarator under the condition that 1) financial and human resources dedicated to this project were very limited, and 2) TESPEL injector was not specially designed according to the TJ-II environment (it was built for the CHS). This successful development is partly attributed to the pellet injection system which consists of highly independent components. Thus the scheme, combining the compact TESPEL injector with the existing pellet injection system could be also applied to the installation of the TESPEL injection system for another experiment device.

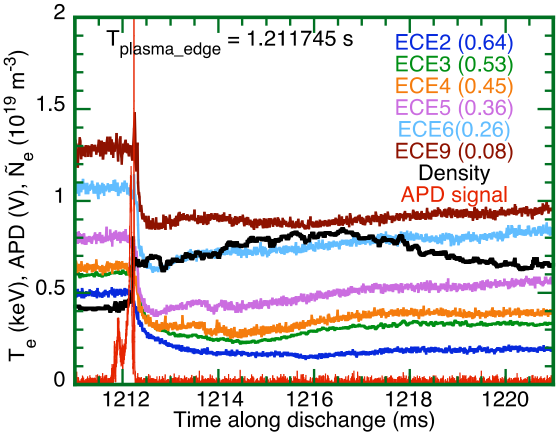

FIG. 3. Time traces of $T_e(\rho)$, $\tilde{N}_e$ and APD output signal about the TESPEL injection time.

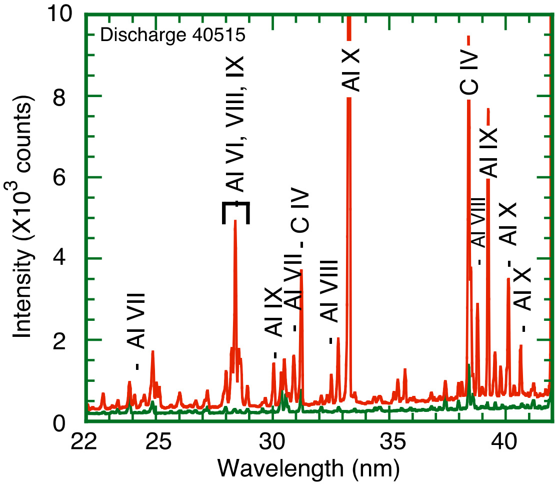

FIG. 4. Spectra from the plasma obtained using the normal incidence spectrometer before (green) and after (red) TESPEL injection. Intense C and Al ion lines are highlighted. The time between recorded spectra is 7.68 ms.

The TESPEL injection experiment on TJ-II will be continued with some improvements. The tracer impurity will be changed to other Z element, e.g. sulfur (S, Z = 16). Because at present there is a strong lack of the spectral data of sulfur in the range of from 20 to 200 nm. The S-TESPEL injection into the TJ-II plasma will contribute to provide such data.

ACKNOWLEDGMENTS

This work is supported by NIFS/NINS under the project of Formation of International Scientific Base and Network (Nos. KEIN1102, and KEIN1104) and by a grant from the Spanish Ministerio de Ciencia y Innovación (Ref. ENE2013-48679-R). N.T. acknowledges support from the Erasmus Mundus Fusion-EP Scholars Program. This work has been carried out within the framework of the EUROfusion Consortium and has received funding from the Euratom research and training programme 2014-2018 under grant agreement No 633053. The views and opinions expressed herein do not necessarily reflect those of the European Commission.

[1] S. Sudo, J. Plasma Fusion Res **69**, 1349 (1993).
[2] S. Sudo and N. Tamura, Rev. Sci. Instrum. **83**, 023503 (2012).
[3] S. Sudo, *et al.*, Plasma Phys. Control. Fusion **55**, 0915014 (2013).
[4] F. J. Casson, *et al.*, Plasma Phys. Control. Fusion **57**, 014031 (2015).
[5] J. Sánchez, *et al.*, Nucl. Fusion **53**, 104016 (2013).
[6] S. Okamura, *et al.*, Nucl. Fusion **39**, 1337 (1999).
[7] S. K. Combs, *et al.*, Fusion Sci. Tech. **64**, 513 (2013).
[8] K. J. McCarthy *et al.*, Proc. Sci. 134 (ECPD2015) (2015).
[9] V. Tribaldos, J. A. Jiménez, J. Guasp, B. Ph. van Milligen, Plasma Phys. Control. Fusion **40**, 2113 (1998).
[10] B. Zurro, *et al.*, Nucl. Fusion **51**, 063015 (2011).